Assignment 1

Boundary layer transition

1.1 Part 1

1.1.1 Airfoil shape calculation

The first airfoil to be investigated belongs to the NACA 4-series. In order to designate it, the 4 digits composing the airfoil name have to be chosen. The first digit is taken equal to 2. The second digit is taken equal to the second digit of the student number, resulting in 5 for 4522249. The last two digit of the airfoil are taken equal to a number N, calculated as the sum of the last three digit of the student number. This results in $N = 2 + 4 + 9 = 15$. As a consequence the designated airfoil is the NACA 2515, which is plotted in 1.1.

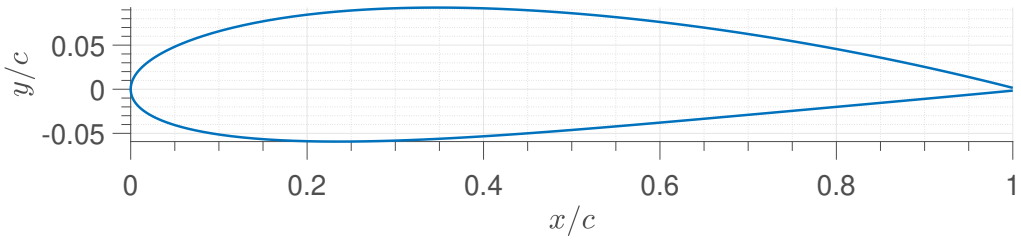

Figure 1.1: Geometry of NACA 2515.

1.1.2 Effect of n-factor on lift and drag polars

Lift and drag polars are calculated considering an angle of attack α between $-2°$ and $10°$, for a Reynolds number $Re = 3.0 \cdot 10^6$. The results obtained for values of n-factor varying from 4 to 12 are shown in Figure 1.2a and they are compared with the inviscid calculation for reference. Two main observations can be made. Firstly, viscosity has the effect of reducing the lift slope in the $c_l - \alpha$ curve w.r.t. an inviscid calculation. Secondly, the variation of n-factor has a substantial impact on the airfoil drag, being this reduced with increasing n-factor for the same c_l. The effect of n-factor on lift is less evident and it is visible only for a specific interval of angles of attack, which is zoomed in Figure 1.2b. Here a non-linearity in the $c_l - \alpha$ curve can be spotted, where the lift slope first increases and then goes back to a lower value. This non-linearity is more evident as the n-factor increases, while is substantially absent for $n = 4$.

The difference in lift and drag at $\alpha = 6.6°$ is further investigated calculating the pressure and skin friction distributions. The inspection of pressure distributions in Figure 1.3a reveals how the curves resulting from viscous calculations are enclosed by the curve obtained with the inviscid calculation, which entails a lower lift for the same angle of attack, as expected. Besides this, very similar results among the different values of n-factor are observed. However, for a region of the top side of the airfoil included between 4% and 15% of the chord a clear difference can be spotted. This is zoomed in Figure 1.3b, where it is possible to notice how the curve associated with the largest value of n-factor lies above the other two until the 14% of the chord, resulting in the additional lift observed previously. Also the curve of $n = 8$ has a portion lying above the curve of $n = 4$, even if also a small trait of the curve lying below is present. In fact the

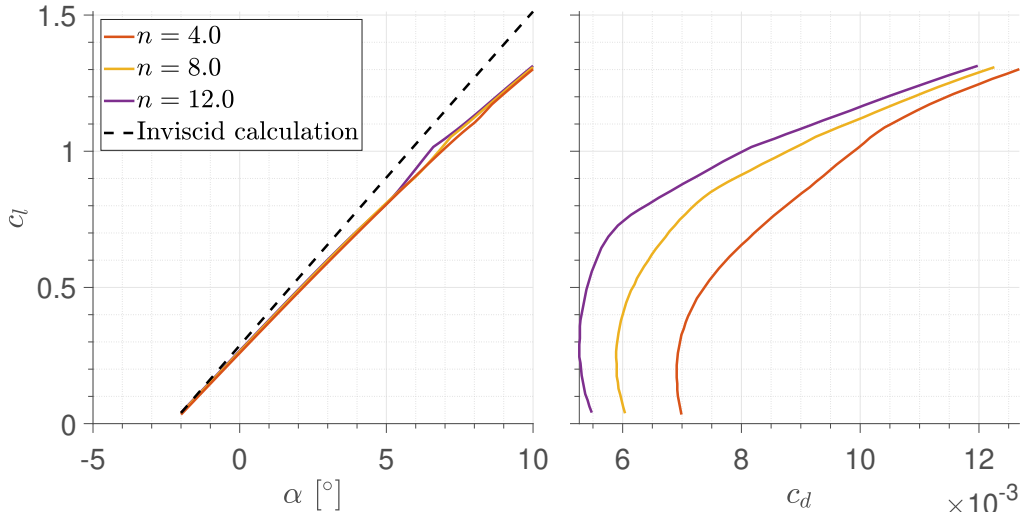

(a) Lift curve (left) and drag polar (right).

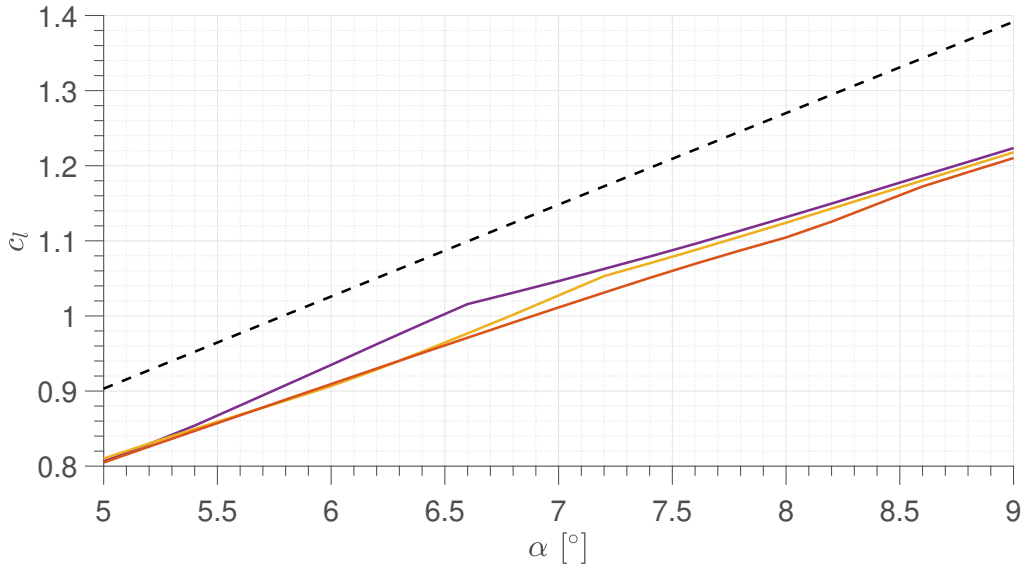

(b) Zoom in on the non-linear part of the lift curve.

Figure 1.2: Effect of n-factor on lift and drag polars of NACA 2515, $Re = 3.0 \cdot 10^6$.

difference in lift observed in Figure 1.2b is small compared w.r.t. to the one observed between $n = 4$ and $n = 12$. Furthermore, all three curves show a small drop in pressure at different points. By looking at Figure 1.4 it is possible to infer that those drops correspond to the transition of laminar to turbulent boundary layer. The distribution of skin friction coefficient C_f is plotted in the figure, which is defined as:

$$C_f = \frac{\tau_w}{\frac{1}{2}\rho_\infty V_\infty^2}, \tag{1.1}$$

where τ_w is the wall shear stress and $1/2\rho_\infty V_\infty^2$ is the dynamic pressure of the free-stream. It is possible to notice how a sharp increase in skin friction is present for the top side of the airfoil in correspondence of the pressure drops observed in Figure 1.3b, meaning that at those locations the boundary layer undergoes transition from laminar to turbulent.

Another observation can be made about the transition location on the top side of the airfoil: this moves towards the leading edge as n decreases, meaning that the boundary layer is more prone to transition. The consequence of an earlier transition to turbulent boundary layer consists in an increase of skin friction drag and thus in overall drag, as it was also observed in Figure 1.2a. One last feature that can be observed in Figure 1.4 is that for $n = 4$ also the bottom side of the airfoil undergoes transition, while this does not happen for the other curves, confirming that small values of n lead to a boundary layer more prone to transition.

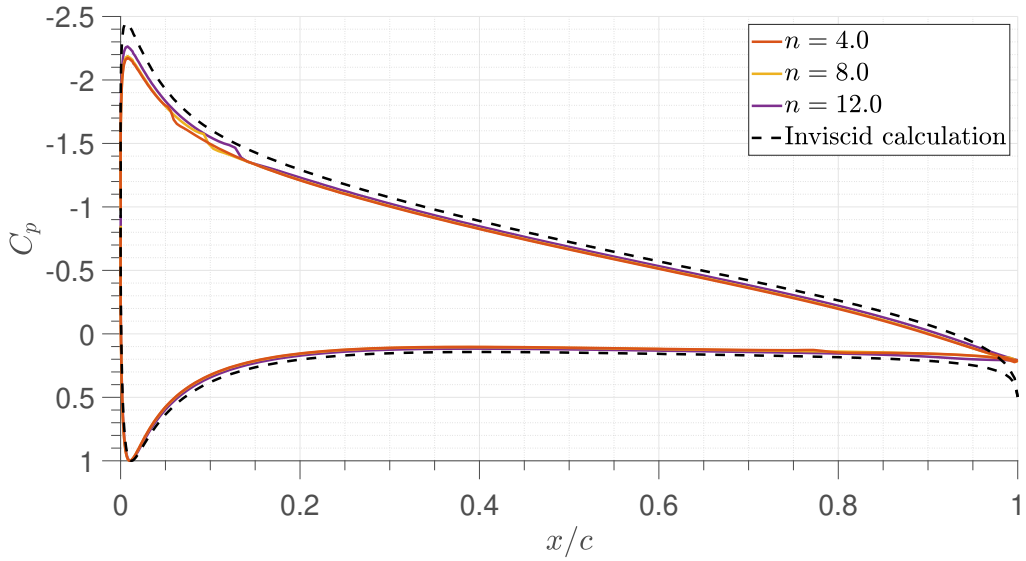

(a) Pressure distribution over the airfoil.

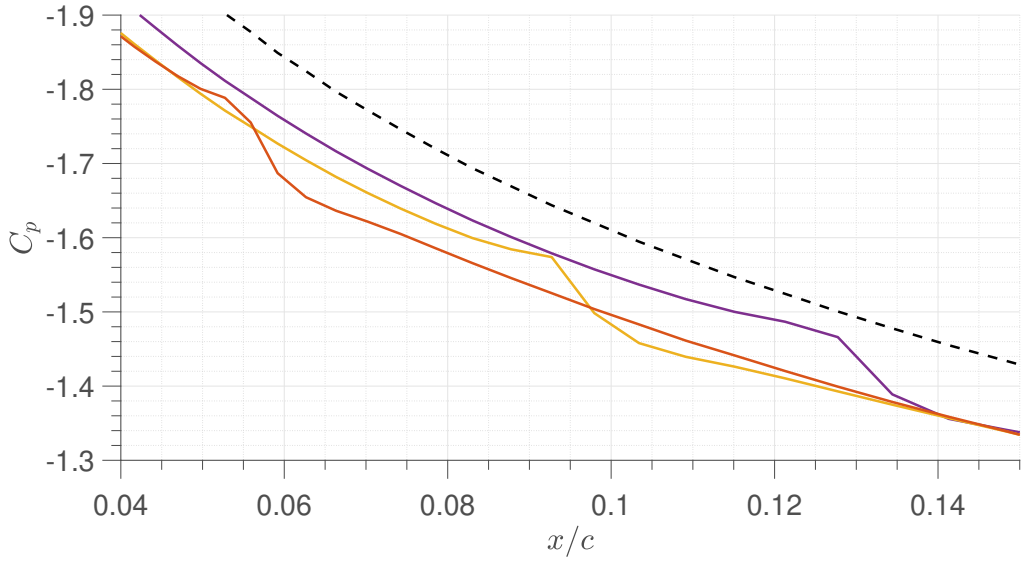

(b) Zoom in on the region of difference in pressure distribution.

Figure 1.3: Effect of n-factor on the pressure distribution over a NACA 2515 at $\alpha = 6.6°$, $Re = 3.0 \cdot 10^6$.

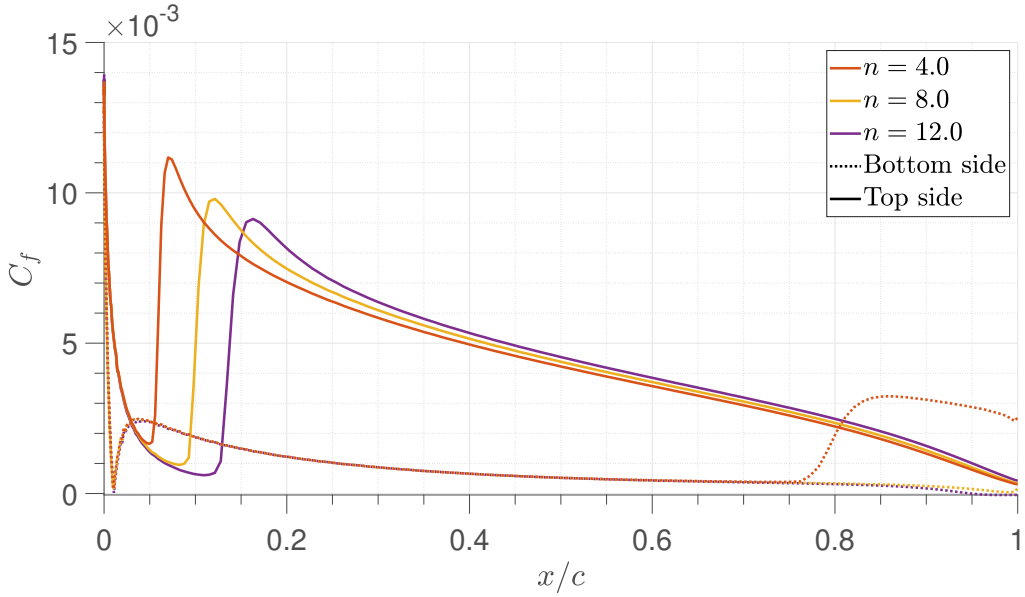

Figure 1.4: Effect of n-factor on the skin friction coefficient over a NACA 2515 at $\alpha = 6.6°$, $Re = 3.0 \cdot 10^6$.

1.2 Part 2

1.2.1 Non-symmetrical airfoil selection

A new airfoil is selected in order to study the effect of the n-factor on the laminar separation bubble. The airfoil must be a non-symmetrical NACA 4-series airfoil and it must show a clearly recognizable laminar separation bubble. The latter is known to be featured on the Eppler 387 airfoil for a Reynolds number in the order of 10^5 [1]. For this reason a NACA 4-series airfoil with similar characteristic to the Eppler 387 is chosen. The maximum camber is taken as 3% of the chord and its position is set at 40% of the chord. Finally, the maximum thickness is chosen to be 9% of the chord, resulting in a NACA 3409. The geometry of such airfoil is shown in Figure 1.5.

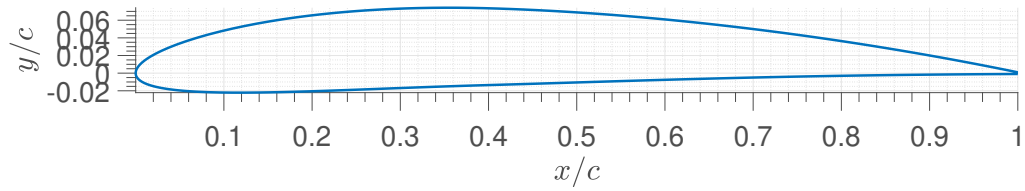

Figure 1.5: Geometry of NACA 3409.

The laminar separation bubble that occurs at an angle of attack of $\alpha = 4°$, Reynolds number of $Re = 5.0{\cdot}10^5$ and $n = 9$ can be observed in Figure 1.6. There both the pressure and the skin friction distributions over the airfoil are shown. The top side of the airfoil exhibits a negative skin friction coefficient from 42% to 47% of the chord, implying the presence of a small separated region, that is to say the laminar separation bubble. For approximately the same interval the pressure distribution is almost a plateau, which is

then followed by a pressure rise over the portion where the transition to a turbulent boundary layer occurs. The characteristic of the laminar separation bubble is that the viscous C_p line lies above the inviscid C_p line for the region where laminar separation occurs. This is caused by the nearly-still fluid in the laminar bubble which cannot sustain a significant pressure gradient and thus makes the pressure distribution close to a plateau.

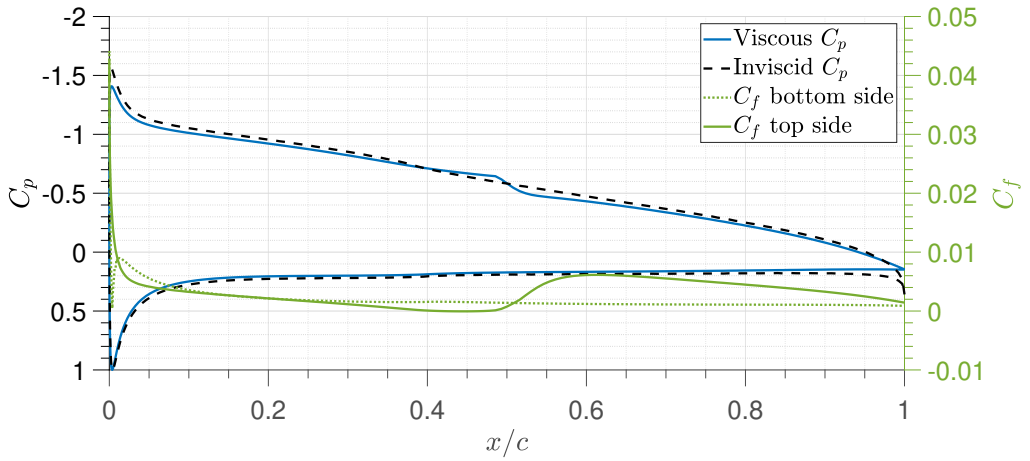

Figure 1.6: Pressure and skin friction distribution over NACA 3409 airfoil, for $\alpha = 4°$, $Re = 5.0 \cdot 10^5$ and $n = 9$.

1.2.2 Effect of n-factor on laminar separation bubble

The effect of n-factor on the length of the separation bubble is investigated for the same angle of attack and Reynolds number of Figure 1.6. Pressure and skin friction distributions over the airfoil are shown in Figure 1.7, for n-factor values varying from 4 to 12. It is possible to observe how the length of the laminar separation bubble increases with n. In fact the separated region in the case of $n = 12$ extends from 34% to 53% of the airfoil while for $n = 9$ it was only from 42% to 47%. As far as the $n = 8$ case is concerned, the skin friction coefficient never reaches a negative value, meaning that full separation never occurs. However, between 42% and 45% the coefficient is in the order of 10^{-5}, implying a region of nearly-still fluid which leads to a pressure distribution over that region that almost resembles a plateau. For $n = 4$ the laminar separation bubble is totally suppressed since the skin friction coefficient stays in the order of 10^{-3} at lowest and the viscous C_p line is never substantially above the inviscid line.

The effect of n-factor on lift and drag coefficient is summarized in Table 1.1. It can be noticed how an increase in n-factor from 4 to 12 entails an increase of lift coefficient of 1.8% and a decrease of drag coefficient of 10.7%. This is qualitatively in agreement with what was observed in Figure 1.2a for NACA 2515, where the n-factor showed a larger effect on the drag coefficient w.r.t. the one on the lift coefficient. Once again the increase in drag has to be ascribed to an earlier transition to turbulent boundary layer, that results in increased skin friction and profile drag compared to laminar flow.

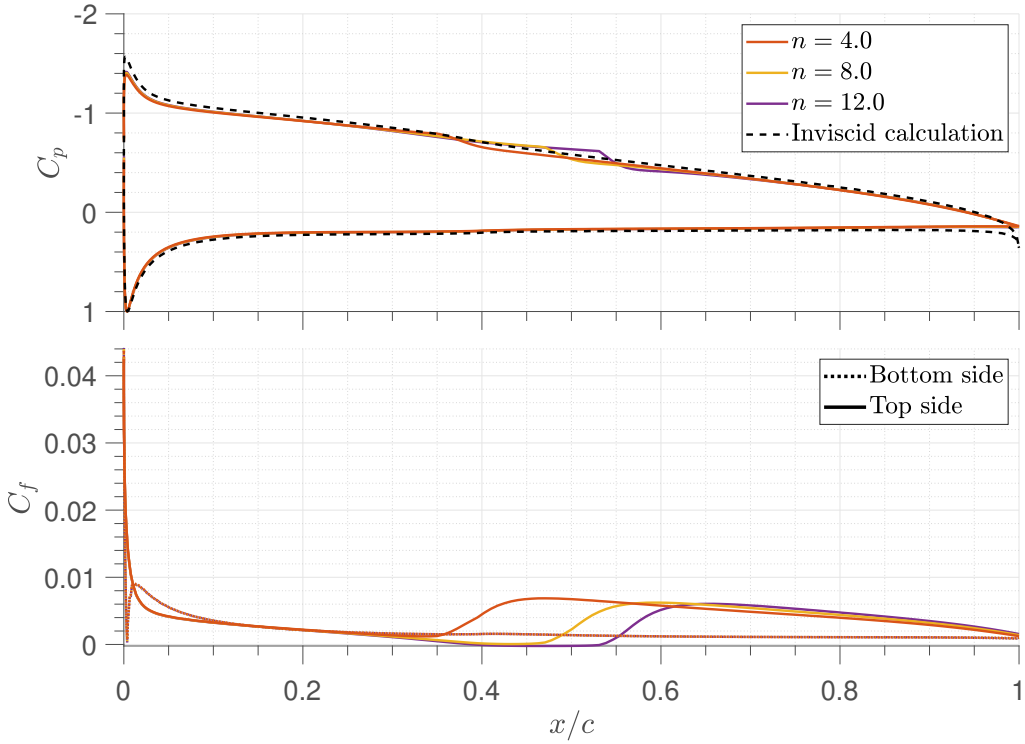

Figure 1.7: Effect of n-factor on pressure (top) and skin friction (bottom) distributions over NACA 3409 airfoil, for $\alpha = 4°$ and $Re = 5.0 \cdot 10^5$.

Table 1.1: Effect of n-factor on lift and drag coefficient of NACA 3409 airfoil, for $\alpha = 4°$ and $Re = 5.0 \cdot 10^5$.

n-factor	Lift coefficient	Drag coefficient
4	0.7803	0.0087
8	0.7887	0.0080
12	0.7941	0.0077

1.2.3 Effect of forced transition

The effect of forced transition is investigated for the same airfoil considering a fixed lift coefficient $c_l = 0.4$ and a Reynolds number $Re = 5.0 \cdot 10^5$. Different forced transition locations for the top side of the airfoil, $x_{tr,top}$, are defined between the leading edge and the location of natural transition. The results in terms of pressure and skin friction distributions are shown in Figure 1.8. It can be observed how a small laminar separation bubble is present only for the free transition case, while it is suppressed for all forced transition cases. Furthermore, as already noticed in the previous figures, transition is observed to lead to a higher level of skin friction and the effect is intensified as transition occurs earlier over the airfoil.

The influence of forced transition on drag coefficient is summarized in Table 1.2. For the lift coefficient and the Reynolds number considered, it appears that drag coefficient

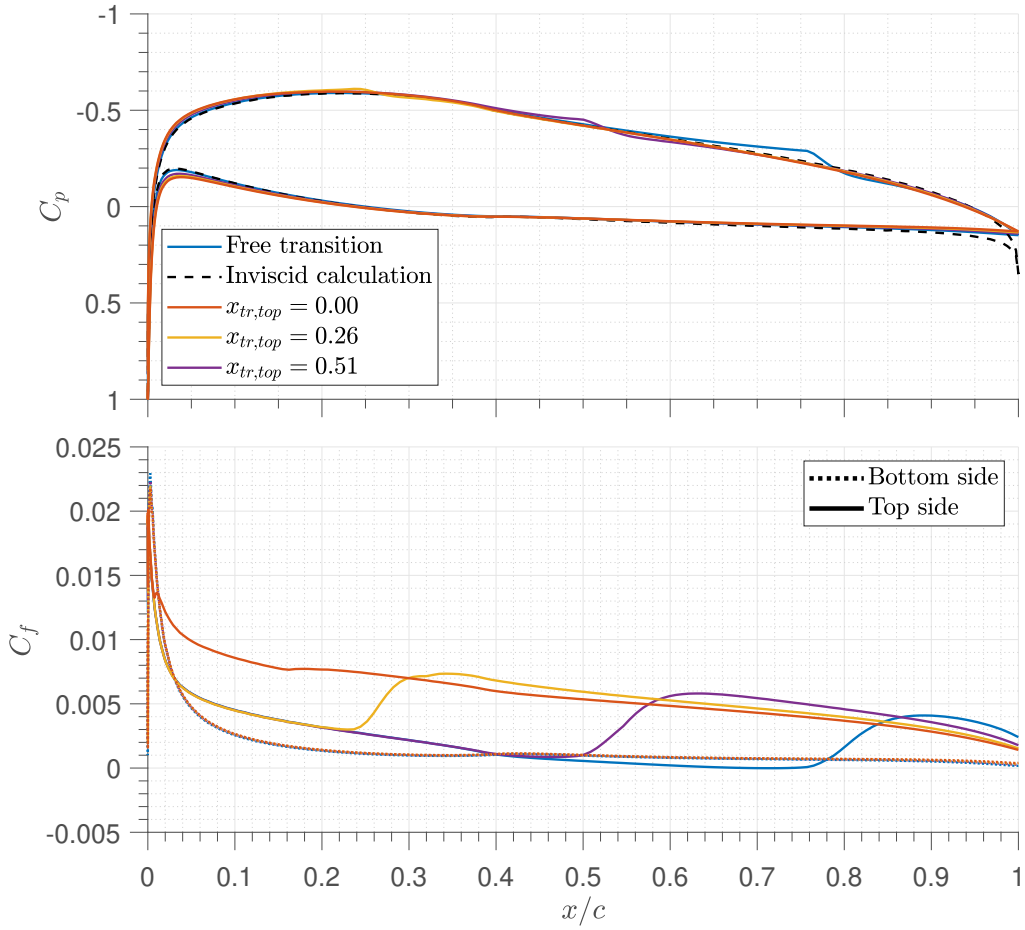

Figure 1.8: Effect of top side forced transition on pressure (top) and skin friction (bottom) distributions over NACA 3409 airfoil, for $c_l = 0.4$ and $Re = 5.0 \cdot 10^5$.

increases as transition is forced earlier than the natural location over the top side of the airfoil. This is in agreement with what is observed in Figure 1.8 for the skin friction distribution.

It is interesting to investigate what happens when the Reynolds number is lowered to $Re = 10^5$, keeping the same lift coefficient. Figure 1.9 shows the pressure and skin friction distributions obtained with the lowered Reynolds number. It can be observed how a substantially longer laminar separation bubble is developed in this case towards the trailing edge of the airfoil. Forced transition suppresses the bubble, as it was also noticed previously.

However, when looking at the effect on drag coefficient it can be observed that forced transition results to be beneficial, leading to a reduction of drag. The largest reduction is obtained when forced transition is applied furthest downstream among the locations considered.

This can be explained by looking at the distribution of momentum thickness θ over the airfoil for both Reynolds numbers $Re = 5.0 \cdot 10^5$ and $Re = 10^5$. The momentum

Table 1.2: Effect of top side forced transition on drag coefficient of NACA 3409 airfoil, for $c_l = 0.4$ and $Re = 5.0 \cdot 10^5$.

Location of top side transition (x/c)	Drag coefficient
0.00 (forced)	0.0097
0.26 (forced)	0.0084
0.51 (forced)	0.0069
0.77 (natural)	0.0057

Table 1.3: Effect of top side forced transition on drag coefficient of NACA 3409 airfoil, for $c_l = 0.4$ and $Re = 10^5$.

Location of top side transition (x/c)	Drag coefficient
0.00 (forced)	0.0159
0.30 (forced)	0.0142
0.60 (forced)	0.0124
0.90 (natural)	0.0161

thickness is defined as [2]:

$$\theta = \int_0^{y_1} \frac{\rho u}{\rho_e u_e} \left(1 - \frac{u}{u_e}\right) \mathrm{d}y \quad \text{for } y_1 \to \infty, \tag{1.2}$$

where u is the streamwise velocity, ρ is the density and the subscript e denotes the free-stream values. Momentum thickness is linked to the momentum deficit due to the presence of the boundary layer. Figure **??** shows the comparison of momentum thickness between the $Re = 5.0 \cdot 10^5$ case and the $Re = 10^5$ case. In the former it can be observed how the level of momentum thickness at the trailing edge when transition is free results to be lower w.r.t. when forced transition is applied. On the contrary, for $Re = 10^5$ momentum thickness of the free transition case undergoes a steep rise towards the leading edge, as a consequence of the presence of the long laminar separation bubble. This causes a momentum deficit in the wake so large that the drag coefficient results to be higher w.r.t. when transition is forced and the laminar bubble is consequently suppressed. This analysis indicates how important is to consider the Reynolds number for the application of forced transition, since it may be either beneficial or detrimental if the Reynolds number is relatively small or large, respectively.

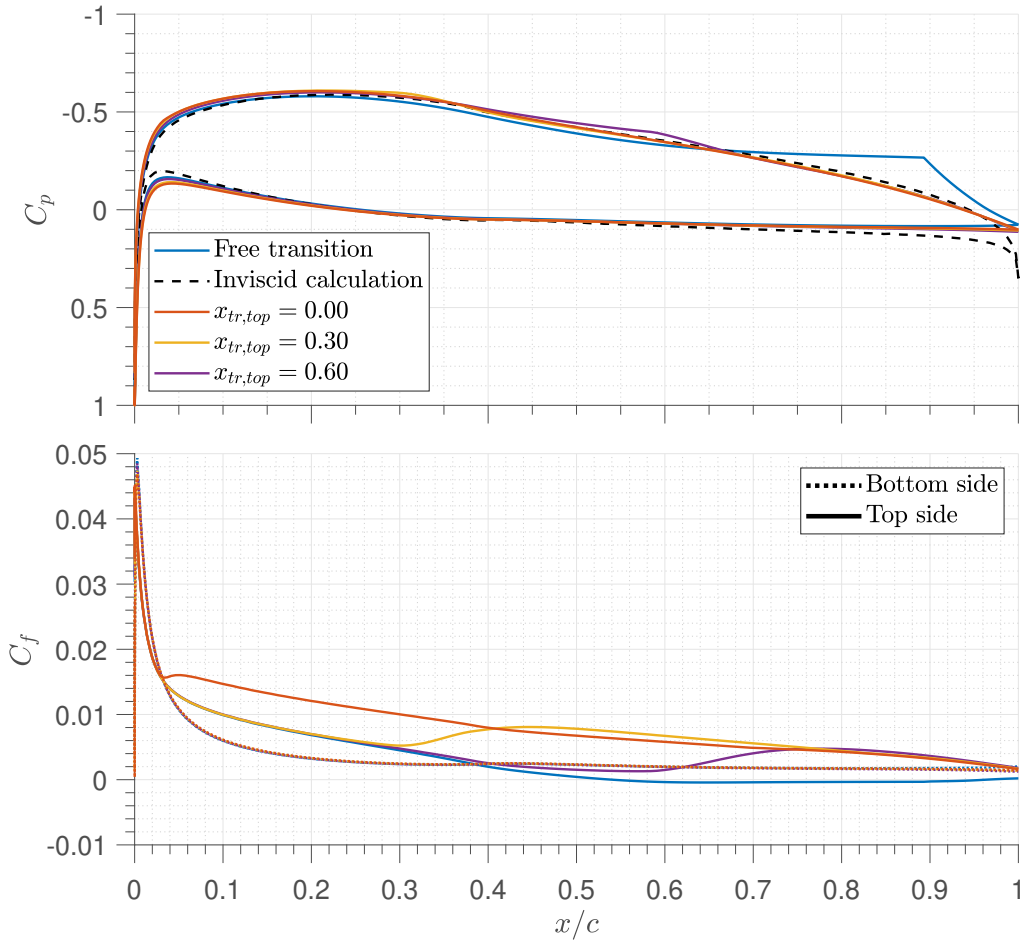

Figure 1.9: Effect of top side forced transition on pressure (top) and skin friction (bottom) distributions over NACA 3409 airfoil, for $c_l = 0.4$ and $Re = 10^5$.

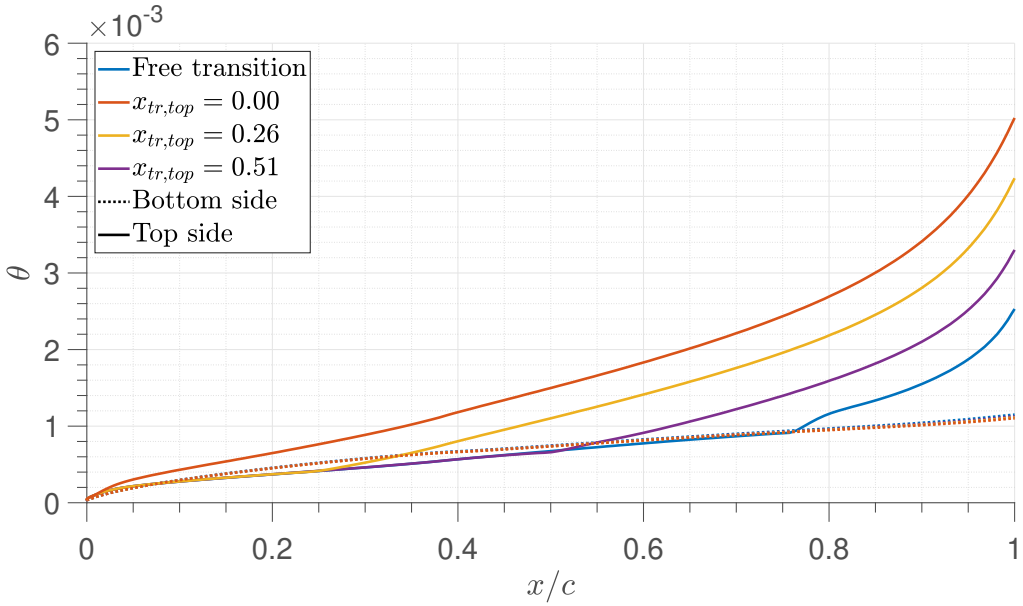

(a) $Re = 5.0 \cdot 10^5$.

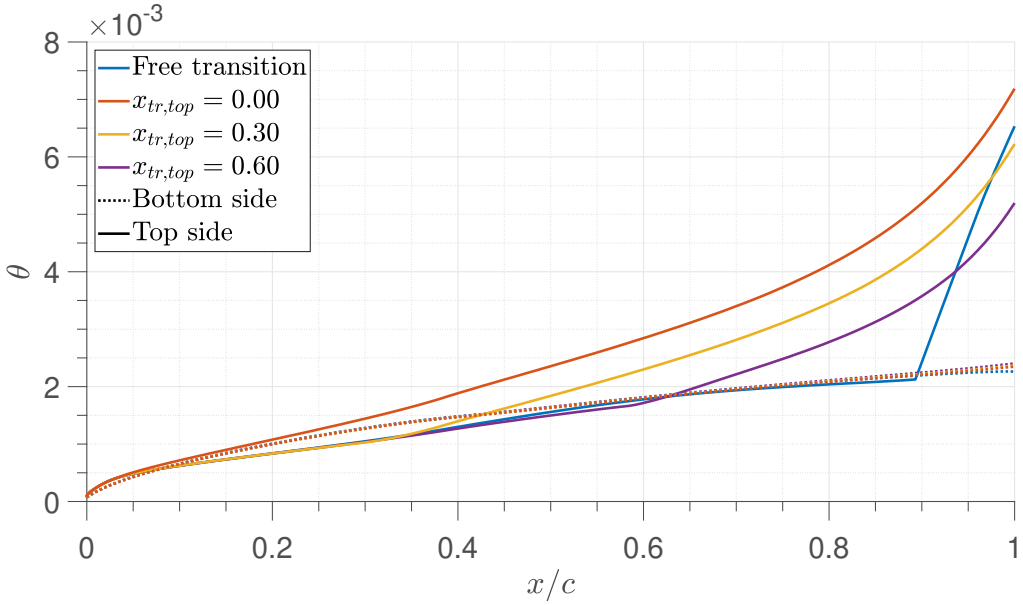

(b) $Re = 10^5$.

Figure 1.10: Effect of top side forced transition on momentum thickness distribution over NACA 3409 airfoil, for $c_l = 0.4$.

References

[1] M. Drela, *Flight Vehicle Aerodynamics*. Cambridge, Massachusetts: The MIT Press, 2014, ISBN: 9780262526449. [Online]. Available: https://books.google.nl/books?id=tffMAgAAQBAJ.

[2] J. D. Anderson Jr., *Fundamental of Aerodynamics*, 5th ed., ser. McGraw-Hill Series in Aeronautical and Aerospace engineering. McGraw-Hill, 2011, ISBN: 9781259010286. [Online]. Available: https://books.google.nl/books?id=xVsiAwAAQBAJ.